Archives of Biochemistry and Biophysics 665 (2019) 12–19

Contents lists available at ScienceDirect

Archives of Biochemistry and Biophysics

journal homepage: www.elsevier.com/locate/yabbi

Biochemical characterization of TyrA dehydrogenases from *Saccharomyces cerevisiae* (Ascomycota) and *Pleurotus ostreatus* (Basidiomycota)

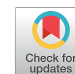

Samuel Lopez-Nieves[a,*,1], Anne Pringle[a,b], Hiroshi A. Maeda[a]

[a] Department of Botany, University of Wisconsin–Madison, Madison, WI, 53706, USA
[b] Department of Bacteriology, University of Wisconsin–Madison, Madison, WI, 53706, USA

ARTICLE INFO

Keywords:
Prephenate dehydrogenase
Arogenate dehydrogenase
Fungi metabolic pathway
Tyrosine biosynthesis

ABSTRACT

L-Tyrosine is an aromatic amino acid necessary for protein synthesis in all living organisms and a precursor of secondary (specialized) metabolites. In fungi, tyrosine-derived compounds are associated with virulence and defense (i.e. melanin production). However, how tyrosine is produced in fungi is not fully understood. Generally, tyrosine can be synthesized via two pathways: by prephenate dehydrogenase ($TyrA_p$/PDH), a pathway found in most bacteria, or by arogenate dehydrogenase ($TyrA_a$/ADH), a pathway found mainly in plants. Both enzymes require the cofactor NAD^+ or $NADP^+$ and typically are strongly feedback inhibited by tyrosine. Here, we biochemically characterized two TyrA enzymes from two distantly related fungi in the Ascomycota and Basidiomycota, *Saccharomyces cerevisiae* (ScTyrA/TYR1) and *Pleurotus ostreatus* (PoTyrA), respectively. We found that both enzymes favor the prephenate substrate and NAD^+ cofactor *in vitro*. Interestingly, while PoTyrA was strongly inhibited by tyrosine, ScTyrA exhibited relaxed sensitivity to tyrosine inhibition. We further mutated ScTyrA at the amino acid residue that was previously shown to be involved in the substrate specificity of plant TyrAs; however, no changes in its substrate specificity were observed, suggesting that a different mechanism is involved in the TyrA substrate specificity of fungal TyrAs. The current findings provide foundational knowledge to further understand and engineer tyrosine-derived specialized pathways in fungi.

1. Introduction

Fungi are rich producers of secondary (or specialized) metabolites [1–4]. Humans have taken advantage of fungal secondary metabolites as pharmaceuticals. For example, the indole alkaloid ergotamine offers relief from migraine attacks, while non-ribosomal peptide cyclosporine is used as an immunosuppressant [5,6]. Aromatic amino acids are the precursor of many secondary metabolites of plants and fungi, such as alkaloids, pigments, and vitamins [7–11]. In the fungal phylum Basidiomycota, tyrosine is the precursor of a unique class of pigments, betalains, only found in the genera of *Amanita* and *Hygrocybe* [12,13] and the plant order Caryophyllales [14]. In the phylum Ascomycota, tyrosine-derived pigments (i.e. melanin) and tyrosine betaine are associated with stress tolerance (e.g. temperature, radiation) and pathogenicity [15–20].

Chorismate, the final product of the shikimate pathway, is the precursor of all three aromatic amino acids, *L*-tryptophan, *L*-phenylalanine, and *L*-tyrosine [7,21]. Chorismate is converted to prephenate, which is used to synthesize phenylalanine and tyrosine via two alternative pathways. In most plants and some bacteria (e.g. α and δ-proteobacteria, spirochaetes), prephenate is first transaminated to produce arogenate, which is oxidatively decarboxylated by $NADP^+$-dependent arogenate dehydrogenase enzyme ($TyrA_a$/ADH, EC 1.3.1.78 and EC 1.3.1.43) to produce tyrosine [22–31]. In contrast, many bacteria first use NAD^+-dependent prephenate dehydrogenase ($TyrA_p$/PDH, EC 1.3.1.12 and EC 1.3.1.13) to convert prephenate into 4-hydroxyphenylpyruvate, which is subsequently transaminated to tyrosine (Fig. 1). However, there are some exceptions to this general pattern and legume plants in particular have both $TyrA_a$/ADH and $TyrA_p$/PDH enzymes [24], whereas some bacteria, such as *Pseudomonas aeruginosa*, have a single TyrA enzyme that can use both arogenate and prephenate substrates and $NADP^+$ as the cofactor [32–34]. Since phenylalanine and tyrosine biosynthesis compete for the prephenate or arogenate precursor, the pathway is highly regulated by feedback inhibition [7,35–39]. However, prior studies have shown that TyrA enzymes are not always inhibited by tyrosine, and some groups of bacteria and plants possess TyrA enzymes that are insensitive or less sensitive to feedback inhibition by tyrosine, including legume $TyrA_p$/PDH enzymes

* Corresponding author.
E-mail address: lopeznieves@wisc.edu (S. Lopez-Nieves).
[1] Current address: Department of Plant Sciences, University of Cambridge, Cambridge, CB2 3EA, UK.

https://doi.org/10.1016/j.abb.2019.02.005
Received 22 November 2018; Received in revised form 6 February 2019; Accepted 12 February 2019
Available online 13 February 2019
0003-9861/ © 2019 Elsevier Inc. All rights reserved.

Abbreviations

$TyrA_p$/PDH prephenate dehydrogenase (also referred to as TYR1)
$TyrA_a$/ADH arogenate dehydrogenase
ScTyrA *Saccharomyces cerevisiae* prephenate dehydrogenase
PoTyrA *Pleurotus ostreatus* prephenate dehydrogenase
EcCM/PDH *Escherichia coli* chorismate mutase/prephenate dehydrogenase

that are completely insensitive to feedback inhibition by tyrosine [23–27,40].

Recently, Schenck et al. [25] identified an active site asparagine 222 (N222) residue in the *Glycine max* $TyrA_p$/PDH (GmPDH1) that is responsible for its prephenate substrate specificity. Mutating the single N222 into an acidic residue (i.e. aspartate, D) in the legume $TyrA_p$/PDH shifted from prephenate to arogenate substrate specificity. The mutation also introduced partial tyrosine sensitivity to otherwise completely insensitive GmPDH1. Introduction of an asparagine (N) residue at the corresponding position in $TyrA_a$/ADH enzymes from non-legume plants [25] and some bacteria [26] also conferred prephenate substrate specificity. Thus, the architecture of the tyrosine biosynthetic pathways can be different between and within taxonomic groups due to the substrate preference of TyrA enzymes, which can be altered by a single mutation in plants and some bacteria.

The tyrosine and phenylalanine biosynthetic pathways have been previously studied in the fungi *Candida maltosa* [41], *Saccharomyces cerevisiae* [42], *Neurospora* sp. [35], and *Claviceps paspali* [43]. These studies detected only prephenate dehydrogenase activity from the protein extracts of these fungal species. The prephenate dehydrogenase activities from crude extracts of *C. maltosa* and *Neurospora* sp. were inhibited by tyrosine but not from those of *S. cerevisiae* and *C. paspali* [41–43]. Although a *TyrA* gene has been reported from *S. cerevisiae* (as *TYR1*) [44], its gene product has not been biochemically characterized. Hence, it is not fully understood how tyrosine is synthesized in fungi.

Here, we characterized recombinant TyrA enzymes from species in two major fungal phyla, Ascomycota and Basidiomycota. The yeast *Saccharomyces cerevisiae* is a model organism of eukaryotes [45,46] while the filamentous fungus *Pleurotus ostreatus* is economically important, not only as an edible mushroom but also because of its ability to degrade lignin [47–49]. We found that tyrosine is produced by the prephenate-specific TyrA enzymes in both organisms; however, their TyrA enzymes showed distinct feedback regulation by tyrosine. Site-directed mutagenesis of the previously-reported residue that confers substrate specificity of plant TyrA enzymes [25,26] did not alter the substrate specificity of ScTyrA, suggesting that as yet unknown amino acid residue(s) is responsible for the substrate specificity of fugal TyrA enzymes.

2. Materials and methods

2.1. Identification of fungal TyrA orthologs

TBLASTN searches were performed using the amino acid sequences of previously characterized plant ADHs (beet BvADHα, KY207372, and BvADHβ, KY207366), the bifunctional enzyme chorismate mutase/prephenate dehydrogenase in *Escherichia coli* (EcCM-PDH, WP_052912694), and the yeast *S. cerevisiae (ScTyrA)* [44], found in the yeast genome (https://www.yeastgenome.org/). The *P. ostreatus* genome deposited in Joint Genome Institute (JGI) (https://jgi.doe.gov/) contained a single *TyrA* gene (thus named *PoTyrA*), which was amplified using gene-specific primers (Table S1) from fresh tissues available in a local supermarket (Madison, WI, USA). Other fungi *TyrA* genes were identified from the National Center for Biotechnology Information (NCBI) and JGI databases. A phylogenetic analysis of predicted TyrA sequences from 83 fungi was performed using MEGA6 (Fig. 2 and S2) [50]. Maximum likelihood analysis was conducted to determine evolutionary distances [51]. The default algorithm and parameters, e.g. a bootstrap method of 1000 replicates using the Jones-Taylor-Thompson model, were used to determine the statistical support for each clade.

2.2. RNA extraction from P. ostreatus and gDNA isolation from E. coli

RNA of *P. ostreatus* was extracted from the mushroom cap of a fresh specimen purchased from a local store by following a previously published method [52]. The RNA was converted into complementary DNA (cDNA) using the High-Capacity cDNA Reverse Transcription Kit (Applied Biosystems, Forester City, CA, USA) using a mix of oligo dT_{20} and random primers. *E. coli* genomic DNA (gDNA) was extracted according to the online protocol "*E. coli* Genomic DNA Extraction" (http://www.bio-protocol.org/e97).

2.3. Recombinant protein expression and purification, and site-directed mutagenesis

The *ScTyrA* gene was synthesized (General Biosystem, Morrisville, NC, USA) and directly cloned into the pET28a vector at *Eco*RI and *Nde*I sites. The full-length coding sequences of *PoTyrA* and *EcCM-PDH* were amplified from cDNA and gDNA, respectively, using gene-specific primers [23]. Both genes were cloned into the same pET28a, in frame with an N-terminal 6x-His-tag using the In-Fusion HD cloning kit and protocol (Clontech, Madison, WI, USA). For site-directed mutagenesis, we followed a previously described method [25]. Amplified DNA was sequenced to confirm that no errors were introduced during the PCR. Recombinant protein expression was performed as previously described, with the exception that protein cultures were grown at 28°C

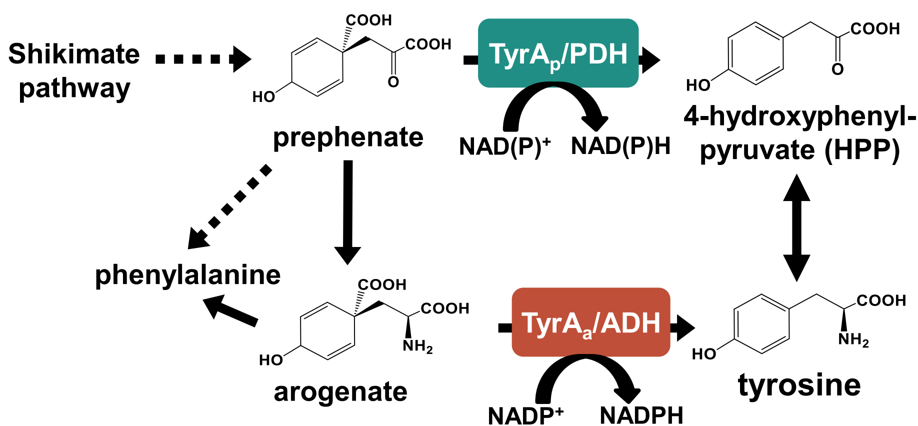

Fig. 1. Tyrosine biosynthetic pathways in different organisms. In most bacteria, prephenate is first decarboxylated via prephenate dehydrogenase ($TyrA_p$/PDH) to form 4-Hydroxyphenylpyruvate (HPP) and then transaminated to form tyrosine. On the other hand, in most plants, tyrosine is synthesized from prephenate via arogenate dehydrogenase ($TyrA_a$/ADH) or prephenate dehydrogenase ($TyrA_p$/PDH), which uses either NAD^+ or $NADP^+$ depending on the organism. Dotted lines represent multiple steps, not explicitly detailed here.

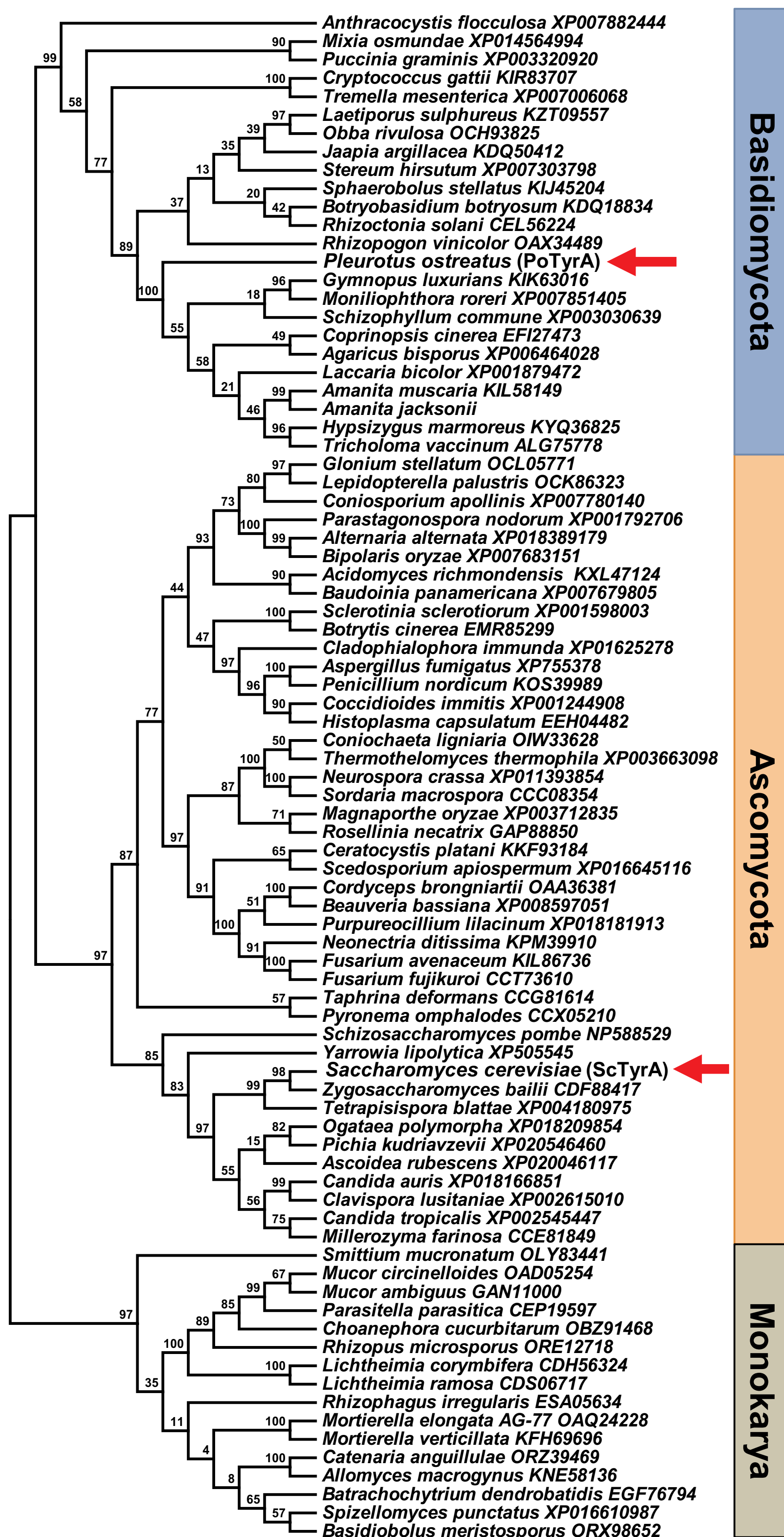

Fig. 2. Unrooted maximum likelihood phylogeny of fungal TyrA enzymes. The tree replicates three of the major groups of fungi: phylum Ascomycota, phylum Basidiomycota and group Monokarya (encompassing Zygomycota, Glomeromycota, Chytridiomycota, Blastocladiomycota) [57]. Red arrows denote ScTyrA and PoTyrA. The accession numbers are listed next to each species. The complete list can be found in Fig. S2. (For interpretation of the references to colour in this figure legend, the reader is referred to the Web version of this article.)

instead of 18°C [23,25,26]. All primers used in this research are shown in Table S1.

2.4. Arogenate and prephenate dehydrogenase activity, tyrosine inhibition assays, and enzyme kinetics

Arogenate and prephenate dehydrogenase enzymatic assays were performed as described previously [23,24] with the exception that both cofactors, NAD^+ and $NADP^+$, were tested. In tyrosine inhibition assays, tyrosine was first dissolved in 0.025 N NaOH at 100 mM. Each inhibition assay contained 500 mM of HEPES (pH 7.6) to maintain the final pH at 7.6. Varying concentrations of tyrosine (final 10 µM - 1 mM) were mixed with 1 mM $NAD(P)^+$ and 0.5 mM prephenate, followed by the addition of TyrA enzyme to start the reactions. The enzymatic activity was measured by monitoring the formation of NAD(P)H at absorbance 340 nm (A_{340nm}) using a spectrophotometer (NanoDrop 2000, Thermo Fisher Scientific, USA) every two minutes for 10 min. Kinetic parameters of the recombinant enzymes were determined from the assays containing varying concentrations of prephenate (39 µM–5 mM) substrate and cofactor NAD^+ in three technical replicates. The reaction was initiated by adding 3.87×10^{-7} and 2.70×10^{-8} g of the ScTyrA or PoTyrA enzymes, as appropriate, into the final 20 µL reactions. A_{340nm} was monitored every nine seconds using a microplate as described previously by Schenck *et al.* 2017 [25].

2.5. Molecular modeling of ScTyrA and PoTyrA

The predicted protein structures of ScTyrA and PoTyrA were modeled by Iterative Threading Assembly Refinement (I-TASSER) [53,54] using the crystal structure of GmPDH1 (PDB # 5T8X) as a template [25]. The predicted model was visualized by PyMOL and predicted amino acid residues that potentially determine the substrate specificity of ScTyrA and PoTyrA were identified (labelled in red on each 3D protein structure, section 3.3).

2.6. Accession numbers

The Genbank accession number for PoTyrA is MG681185.

3. Results and discussion

3.1. ScTyrA and PoTyrA have only prephenate dehydrogenase activity and prefer NAD^+ as the cofactor

Plant TyrA enzymes and closely related spirochaetes and proteobacteria TyrAs have arogenate dehydrogenase activity [26,55,56]; however, the substrate specificity of fungal TyrA enzymes, which belong to a distinct clade that house other bacteria and archaea groups [26,56], is currently unknown. Unlike plants, which have multiple

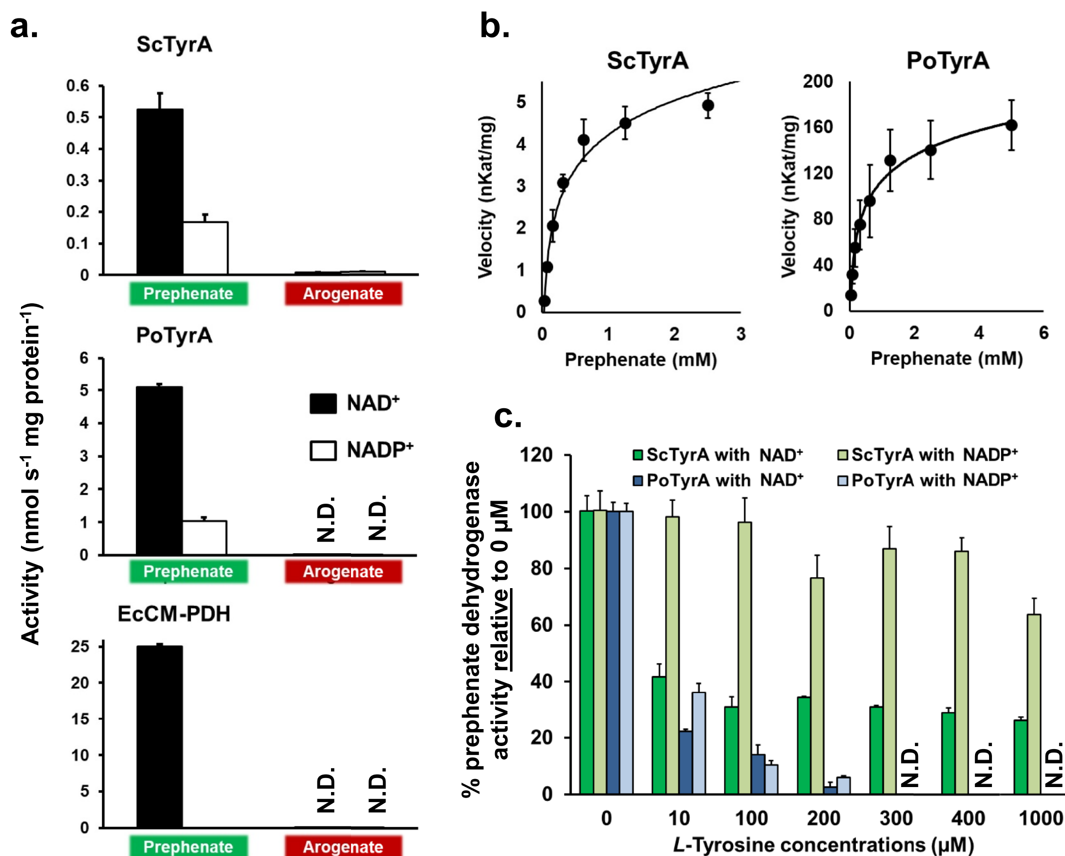

Fig. 3. Biochemical characterization of ScTyrA and PoTyrA enzymes. (**a**) Substrate and cofactor specificity of ScTyrA and PoTyrA. EcCM-PDH was used as control for the experiment. Prephenate and arogenate dehydrogenase activity of ScTyrA, PoTyrA, and EcCM-PDH using either NAD^+ or $NADP^+$ at 37 °C for 10 min. ScTyrA and PoTyrA prefer prephenate as the substrate and NAD^+ as the cofactor. Unlike *E. coli* TyrA, fungal TyrAs are also able to produce tyrosine with the cofactor $NADP^+$. Bars are average specific activity expressed at nmol s^{-1} mg $protein^{-1}$ ± s.e.m. with n = 3 replications. (**b**) Michaelis-Menten plots of recombinant TyrA enzymes. Kinetic assay portrays the results of steady-state kinetic analyses with prephenate as the substrate and NAD^+ as cofactor. Data are the mean reaction velocity (nkat mg $protein^{-1}$) ± s.e.m. with n ≥ 3 replicates at each substrate concentration (mM). The experimentally determined kinetic parameters, shown in Table 1, were used to generate Michaelis-Menten kinetic curves. (**c**) Inhibition of ScTyrA and PoTyrA by tyrosine. Prephenate dehydrogenase activity was measured at different tyrosine concentrations using both NAD^+ and $NADP^+$ cofactors and purified recombinant enzymes of ScTyrA and PoTyrA. Data are expressed as the percentage of respective control activity without tyrosine (0 µM) and the means of three independent experiments ± s.e.m. are plotted. N.D. = Not detectable.

copies of *TyrA* genes, only a single *TyrA* candidate gene was found in the genomes of the 83 fungal species available from the NCBI or *yeastgenome*. Phylogenetic analysis of the predicted fungal *TyrA* genes identified three distinct fungal clades: Basidiomycota, Ascomycota, and Monokarya (Zygomycota, Chytridiomycota, Blastocladiomycota, Fig. 2), consistent with the taxonomic relationships of these fungal species [57].

Representative basidiomycete and ascomycete TyrAs, from *S. cerevisiae* and *P. ostreatus*, respectively, were selected and biochemically characterized. The recombinant enzymes of ScTyrA and PoTyrA were expressed in *E. coli*, purified using affinity chromatography, and analyzed for arogenate and prephenate dehydrogenase activities. The *E. coli* EcCM-PDH enzyme was used as a control; it has prephenate but not arogenate dehydrogenase activity and a strong preference towards the NAD^+ cofactor [29,58]. Similar to *E. coli* EcCM-PDH, both ScTyrA and PoTyrA showed prephenate dehydrogenase activity and preferred the NAD^+ cofactor. Unlike EcCM-PDH, ScTyrA and PoTyrA also showed some activity with the $NADP^+$ cofactor, though weaker than with NAD^+ (Fig. 3a). Neither the *E. coli* nor the fungal PoTyrA enzymes exhibited detectable arogenate dehydrogenase activity, but very low activity was detected for the fungal ScTyrA enzyme (0.067 and 0.009 nmol s^{-1} mg protein^{-1} for NAD^+ and $NADP^+$, respectively (Fig. 3a). The near lack of arogenate dehydrogenase activity in the fungal TyrA enzymes (Fig. 3a) suggests that fungi produce tyrosine predominately by prephenate dehydrogenase, similar to what has been described for many bacteria [26,28,29,37–39].

The specific activity of PoTyrA (5 and 1 nmol s^{-1} mg protein^{-1} with NAD^+ and $NADP^+$, respectively) was higher than that of ScTyrA (0.5 and 0.2 nmol s^{-1} mg protein^{-1}, respectively) when prephenate was used as the substrate. However, the specific activity of both enzymes was lower than that of EcCM-PDH (24.97 with NAD^+ and 0.76 nmol s^{-1} mg protein^{-1} with $NADP^+$, Fig. 3a) and of previously reported TyrA enzymes having prephenate dehydrogenase activity [24,25,58,59]. The kinetic analyses of ScTyrA and PoTyrA using prephenate and NAD^+ showed similar K_m values for prephenate, 0.25 and 0.32 mM, respectively (Fig. 3b; Table 1), values that are similar to previously reported K_m value from the fungus *Candida maltosa* (K_m = 0.22 mM) [41]. The K_m values of ScTyrA and PoTyrA were, however, similar to those of previously characterized TyrA enzymes from bacteria and plants, which range from 0.017 to 3.3 mM and 0.077–0.223 mM, respectively [24–26,30,32,37,60–64]. PoTyrA had a turnover rate thirty times higher than that of ScTyrA (k_{cat} of 0.1 vs. 3.1 s^{-1}, respectively, Fig. 3b; Table 1).

3.2. ScTyrA is less sensitive to tyrosine than PoTyrA

To test if the fungal TyrA enzymes are feedback inhibited by tyrosine, like many other TyrAs [22–24,30,36,37,41,59,60], prephenate dehydrogenase activity was measured in the presence and absence of different concentrations of tyrosine. The activity of PoTyrA was completely inhibited at and beyond 200 μM tyrosine using either cofactors, NAD^+ or $NADP^+$. By contrast, ScTyrA showed a relaxed sensitivity to tyrosine-mediated inhibition: ScTyrA still exhibited 30 and 60% of activity with NAD^+ and $NADP^+$, respectively, even at 1 mM tyrosine (Fig. 3c). This result is consistent with a previous report from *S. cerevisiae* yeast crude extracts that also showed prephenate dehydrogenase activity with relaxed sensitivity to tyrosine inhibition [42].

A recent study demonstrated that in the plant order Caryophyllales the presence of a deregulated TyrA enzyme was tightly linked to the occurrence of tyrosine-derived specialized metabolites, betalain pigments [23]. Thus, the relaxed regulation of TyrA and hence tyrosine biosynthesis in *S. cerevisiae*, and potentially in related species, might be linked to an extra demand of tyrosine for the production of downstream secondary metabolites derived from tyrosine.

3.3. Protein structure alignments predict the $NAD(P)^+$ binding site and potential residue responsible for substrate specificity of SoTyrA and PoTyrA

Amino acid sequence comparisons revealed ScTyrA and PoTyrA have ~50% similarity between them but are only ~25% similar to plant TyrAs (i.e. BvADHα, AtADH2, GmPDH1) and ~20% similar to bacterial TyrAs such as from *Escherichia coli*, *Aquifex aeolicus*, and *Synechocystis* sp. PCC6803 (Fig. S1). An alignment of all fungal TyrA proteins identified highly-conserved residues responsible for $NAD(P)^+$ binding (GxGxxG motif) [55] and catalysis (e.g. Ser107 and His130, according to legume TyrAs) [25,65] (Figs. S2 and S3). The residues responsible for NAD^+ *versus* $NADP^+$ cofactor specificity are located between 11 and 19 residues downstream of the GxGxxG motif [25,55]. Bacterial TyrAs, which exhibit a strong preference for NAD^+ (e.g. *E. coli* CM-PDH, Fig. 3a) [29], have a conserved Asp residue at position 39, while organisms with a strong preference for $NADP^+$ have Gly, Ala, Ser, or Thr before a conserved Arg residue [(G,A,S,T)R]. On the other hand, bacteria TyrAs with broad cofactor specificity have Gly followed by two random residues before the conserved Arg (GxxR) [25,55]. Similarly, fungal TyrAs have Gly at position ~37 (or position ~43, depending on the fungal group), followed by Trp, Arg or Lys or Gln, and then finish with a conserved residue [GW(R,K,Q)x] at position ~42 (or ~46 depending on the fungal group, Fig. S3). Thus, these results are consistent with the broad cofactor specificity of ScTyrA and PoTyrA (Fig. 3a).

The fungal TyrAs also possess an active site asparagine residue at position 234, Asn (N) 234 (the position numbering based on ScTyrA and PoTyrA), that potentially confer prephenate substrate specificity, as in the TyrA enzymes of plants and bacteria that are closely-related to plants (Fig. S3) [25,26]. Structure models of ScTyrA and PoTyrA (Fig. S4) provide an additional support that N234 in the fungal TyrA enzymes corresponds to the N222 residue in the crystal structure of the *Glycine max* PDH1 (Fig. S4). Most fungal TyrAs have Asn (N) residue at the corresponding position 234, with some exceptions: Gln (Q), Ser (S), and Ala (A), but not with an acidic Asp (D) residue (Fig. S3), that would confer arogenate substrate specificity [25,26]. The comparisons among the sequences suggest that N234 may determine prephenate specificity also in fungal TyrA enzymes, like in plants and closely related bacteria.

To experimentally test this hypothesis, site-directed mutagenesis was performed on ScTyrA and PoTyrA to convert Asn234 into Asp234 (the N234D mutation). The mutant enzymes, ScTyrA_N234D and PoTyrA_N234D, were expressed in *E. coli* and purified similarly to the wild type enzyme. Neither of the N234D mutant enzymes of ScTyrA or PoTyrA, however, showed arogenate dehydrogenase activity, although the prephenate dehydrogenase activity was slightly reduced in ScTyrA_N234D while that of PoTyrA_N234D increased by 5 times relative to the respective wild type enzyme (Fig. 4a). PoTyrA_N234D did not alter its tyrosine sensitivity and was still completely inhibited at or beyond 100 μM tyrosine, while ScTyrA_N234D exhibited relaxed sensitivity to tyrosine, similar to the wild type ScTyrA enzyme (Fig. 4b).

Table 1
Kinetics parameters of fungal TyrA enzymes.

	Substrate[a]	K_m (mM)	V_{max} (nkat mg protein^{-1})	k_{cat} (s^{-1})	k_{cat}/K_m (mM^{-1} s^{-1})
ScTyrA	prephenate	0.25 ± 0.04	5.26 ± 0.33	0.10 ± 0.01	2.62 ± 0.71
PoTyrA	prephenate	0.32 ± 0.08	174.77 ± 25.77	3.09 ± 0.45	204.33 ± 105.44

[a] Kinetic parameters could not be obtained using arogenate substrate due to the low or lack of activity (Fig. 3).

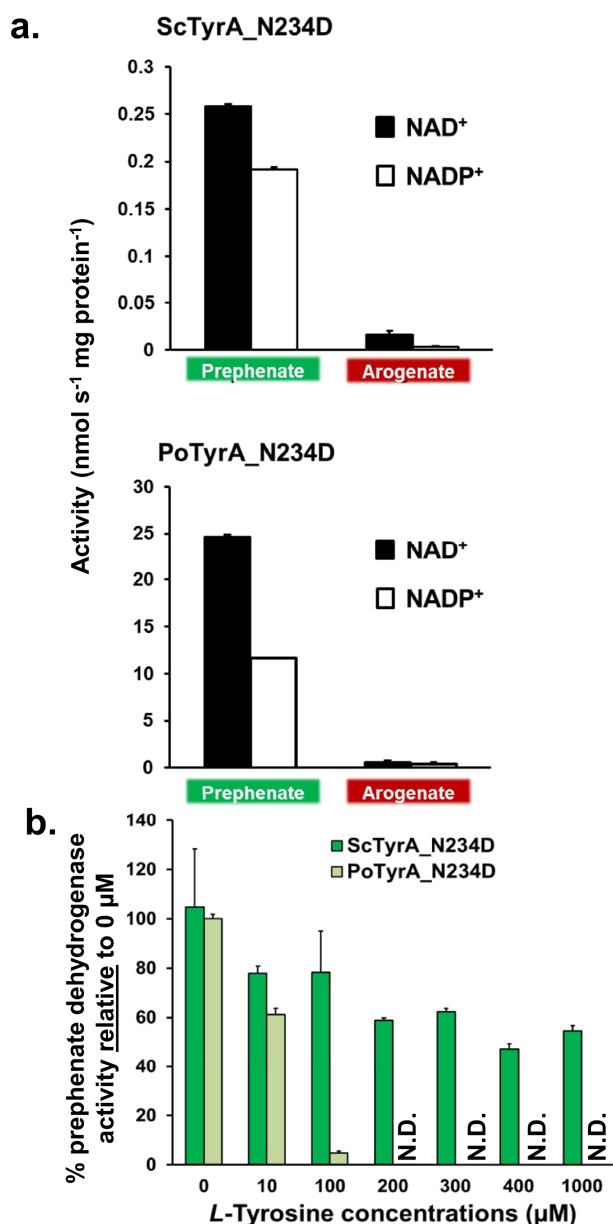

Fig. 4. Site directed mutagenesis of ScTyrA and PoTyrA. (**a**) Enzyme activities and substrate specificities of ScTyrA_N234D and PoTyrA_N234D. Prephenate and arogenate dehydrogenase activities of the ScTyrA_N234D and PoTyrA_N234D mutants using NAD^+ or $NADP^+$ were measured at 37 °C for 10 min. The N234D mutation does not impact ScTyrA or PoTyrA substrate specificity. Bars are average specific activity (nmol s^{-1} mg $protein^{-1}$) ± s.e.m. with n = 3 replications. (**b**) Tyrosine inhibition assays of ScTyrA_N234D and PoTyrA_N234D using the NAD^+ cofactor. Prephenate dehydrogenase activity was measured in the absence and presence of different tyrosine concentrations. N.D. = Not detectable. The specific mutation in the predicted protein model as well as the structural alignment of the fungal TyrA with GmPDH1 can be found in Fig. S4.

These results suggest that the N234 residue is not responsible for the substrate specificity and tyrosine sensitivity of fungal TyrA enzymes, unlike in TyrAs of plants and closely related bacteria [25,26,63] and yet an unknown mechanism is involved in the substrate specificity of fungal TyrA enzymes.

Although overall TyrA enzyme structures seem to be conserved between plant and fungal TyrAs (Fig. S4), their active site architectures may be different, given that TyrA enzymes from fungi and plants (and closely related bacteria) belong to distinct clades (clade I and II, respectively) [26]. Mutagenesis studies identified additional residues involved in the tyrosine inhibition of bacterial TyrA enzymes from *E. coli* and *Aquifex aeolicus* [27,36,61] (H257 and H217 in *E. coli* and *A. aeolicus*, respectively), which also belong to the clade II. Thefore, potential roles of the corresponding residues, H191 and H193 for ScTyrA and PoTyrA, respectively (Fig. S3) could be tested in future studies. However, residues responsible for prephenate vs. arogenate substrate specificity are currently unknown in the clade II, including fungal TyrA enzymes.

Fungi and plants produce a tremendous array of natural products, many of which provide critical and diverse chemical resources to the human society [1,2]. The current study provides fundamental knowledge about the pathway architecture and regulation of biosynthesis of tyrosine, a key precursor of numerous natural products with nutritional and pharmaceutical values [7,11,66]. While two distantly-related fungi have prephenate-specific $TyrA_p$/PDH enzymes (Fig. 3a), ScTyrA but not PoTyrA exhibits relaxed sensitivity to tyrosine-mediated feedback regulation (Fig. 3c), which often limits the production of tyrosine and its downstream products. Recent advancements in synthetic biology enable reconstruction of various plant specialized metabolic pathways in yeast for heterologous production of opioids, artemisinin, resveratrol, *p*-coumarate, and betalain pigments [66–74]. While the metabolic and physiological functions of the deregulation of ScTyrA in yeast remain to be investigated, our findings provide important baseline information for further optimizing the tyrosine precursor supply in different fungi: For example, deregulating the feedback inhibition or enhancing the turnover rate of the TyrA-catalyzed step will likely improve tyrosine production in *P. ostreatus* and *S. cerevisiae*, respectively. Further understanding of the endogenous mechanisms for the supply of key precursor molecules (e.g. tyrosine) in different fungal hosts will provide rationale strategies to achieve sizable production of downstream natural products.

Conflicts of interest statement

The authors declare no conflict of interest.

Acknowledgements

We thank Bastien Bennetot for his assistance in recombinant protein isolation. This work was supported by the National Science Foundation grant IOS-1354971 and an Agriculture and Food Research Initiative competitive grant (2015-67013-22955) from the USDA National Institute of Food and Agriculture to H.A.M. S.L.N. was partly supported by the National Science Foundation Graduate Research Fellowship (Grant No. DGE-1256259) and an Advanced Opportunity Fellowship (AOF) from the University of Wisconsin-Madison.

Appendix A. Supplementary data

Supplementary data to this article can be found online at https://doi.org/10.1016/j.abb.2019.02.005.

References

[1] N.P. Keller, G. Turner, J.W. Bennet, Fungal secondary metabolism - from biochemistry to genomics, Nat. Rev. Microbiol. 12 (2005) 937–947.
[2] J. Macheleidt, D.J. Mattern, J. Fischer, T. Netzker, J. Weber, V. Schroeckh, V. Valiante, A.A. Brakhage, Regulation and role of fungal secondary metabolites, Annu. Rev. Genet. 50 (2016) 371–392.
[3] J.C. Nielsen, J. Nielsen, Development of fungal cell factories for the production of secondary metabolites: linking genomics and metabolism, Synth. Syst. Biotechnol. 2 (2017) 5–12.
[4] M. Stadler, D. Hoffmeister, Fungal natural products-the mushroom perspective, Front. Microbiol. 6 (2015) 1–4.
[5] J.J. Chen, M.Y. Han, T. Gong, J.L. Yang, P. Zhu, Recent progress in ergot alkaloid research, RSC Adv. 7 (2017) 27384–27396.

[6] C. Schultz, Safety and efficacy of cyclosporine in the treatment of chronic dry eye, Ophthalmol. Eye Dis. 6 (2014) 37–42.
[7] H. Maeda, N. Dudareva, The shikimate pathway and aromatic amino acid biosynthesis in plants, Annu. Rev. Plant Biol. 63 (2012) 73–105.
[8] R. Bentley, The shikimate pathway - a metabolic tree with many branches, Crit. Rev. Biochem. Mol. Biol. 25 (1990) 307–384.
[9] J.L. Rubin, R. a Jensen, Enzymology of *L*-tyrosine biosynthesis in mung bean (*Vigna radiata* [L.] Wilczek), Plant Physiol. 64 (1979) 727–734.
[10] R.A. Jensen, D.A. Pierson, Evolutionary implications of different types of microbial enzymology for *L*-tyrosine biosynthesis, Nature 254 (1975) 667–671.
[11] C.A. Schenck, H.A. Maeda, Tyrosine biosynthesis, metabolism, and catabolism in plants, Phytochem 149 (2018) 82–102.
[12] H. Musso, The pigments of fly agaric, *Amanita muscaria*, Tetrahedron 35 (1979) 2843–2853.
[13] R. Von Ardenne, H. Döpp, H. Musso, W. Steiglich, Über das vorkommen von muscaflavin bei hygrocyben (Agaricales) und seine dihydroazepin-struktur, Z Naturforsch C 29C (1974) 637–639.
[14] S.F. Brockington, R.H. Walker, B.J. Glover, P.S. Soltis, D.E. Soltis, Complex pigment evolution in the Caryophyllales, New Phytol. 190 (2011) 854–864.
[15] E.S. Jacobson, Pathogenic roles for fungal melanins, Clin. Microbiol. Rev. 13 (2000) 708–717.
[16] C.A. Carollo, A.L.A. Calil, L.A. Schiave, T. Guaratini, D.W. Roberts, N.P. Lopes, G.U.L. Braga, Fungal tyrosine betaine, a novel secondary metabolite from conidia of entomopathogenic *Metarhizium* spp. fungi, Fungal Biol 114 (2010) 473–480.
[17] C. Ghazaei, Molecular insights into pathogenesis and infection with *Aspergillus fumigatus*, Malays. J. Med. Sci. 24 (2017) 10–20.
[18] C.M. Marcos, H.C. de Oliveira, W. de C.M.A. de Melo, J. de F. da Silva, P.A. Assato, L. Scorzoni, S.A. Rossi, A.C.A. de Paula e Silva, M.J.S. Mendes-Giannini, A.M. Fusco-Almeida, Anti-immune strategies of pathogenic fungi, Front. Cell. Infect. Microbiol. 6 (2016) 142.
[19] J.E. Hallsworth, N. Magan, Culture age, temperature, and pH affect the polyol and trehalose contents of fungal propagules, Appl. Environ. Microbiol. 62 (1996) 2435–2442.
[20] S. bhatia, K. Sharma, A. Sharma, A. Garg, S. Kumar, A. Purohit, Mycosporine and mycosporine-like amino acids: a paramount tool against ultra violet irradiation, Pharmacogn. Rev. 5 (2011) 138–146.
[21] G.H. Braus, Aromatic amino acid biosynthesis in the yeast *Saccharomyces cerevisiae*: a model system for the regulation of a eukaryotic biosynthetic pathway, Microbiol. Rev. 55 (1991) 349–370.
[22] P. Rippert, M. Matringe, Molecular and biochemical characterization of an *Arabidopsis thaliana* arogenate dehydrogenase with two highly similar and active protein domains, Plant Mol. Biol. 48 (2002) 361–368.
[23] S. Lopez-Nieves, Y. Yang, A. Timoneda, M. Wang, T. Feng, S.A. Smith, S.F. Brockington, H.A. Maeda, Relaxation of tyrosine pathway regulation underlies the evolution of betalain pigmentation in Caryophyllales, New Phytol. 217 (2018) 896–908.
[24] C.A. Schenck, S. Chen, D.L. Siehl, H.A. Maeda, Non-plastidic, tyrosine-insensitive prephenate dehydrogenases from legumes, Nat. Chem. Biol. 11 (2015) 52–57.
[25] C.A. Schenck, C.K. Holland, M.R. Schneider, Y. Men, S.G. Lee, J.M. Jez, H.A. Maeda, Molecular basis of the evolution of alternative tyrosine biosynthetic routes in plants, Nat. Chem. Biol. 13 (2017) 1029–1035.
[26] C.A. Schenck, Y. Men, H.A. Maeda, Conserved molecular mechanism of TyrA dehydrogenase substrate specificity underlying alternative tyrosine biosynthetic pathways in plants and microbes, Front Mol Biosci 4 (2017) 73.
[27] P. Legrand, R. Dumas, M. Seux, P. Rippert, R. Ravelli, J.L. Ferrer, M. Matringe, Biochemical characterization and crystal structure of *Synechocystis* arogenate dehydrogenase provide insights into catalytic reaction, Structure 14 (2006) 767–776.
[28] J. Bonvin, R.A. Aponte, M. Marcantonio, S. Singh, D. Christendat, J.L. Turnbull, Biochemical characterization of prephenate dehydrogenase from the hyperthermophilic bacterium *Aquifex aeolicus*, Protein Sci. 15 (2006) 1417–1432.
[29] G.S. Hudson, V. Wong, B. Davidson, Chorismate mutase/prephenate dehydrogenase from *Escherichia coli* K12: purification, characterization, and identification of a reactive cysteine, Biochemistry 23 (1984) 6240–6249.
[30] S. Lim, J.R. Springstead, M. Yu, W. Bartkowski, I. Schröder, H.G. Monbouquette, Characterization of a key trifunctional enzyme for aromatic amino acid biosynthesis in *Archaeoglobus fulgidus*, Extremophiles 13 (2009) 191–198.
[31] S.L. Stenmark, D.L. Pierson, R.A. Jensen, G.I. Glover, Blue-Green bacteria synthesise *L*-tyrosine by the pretyrosine pathway, Nature 247 (1974) 290–292.
[32] T. Xia, R.A. Jensen, A single cyclohexadienyl dehydrogenase specifies the prephenate dehydrogenase and arogenate dehydrogenase components of the dual pathways to *L*-tyrosine in *Pseudomonas aeruginosa*, J. Biol. Chem. 265 (1990) 20033–20036.
[33] A.M. Fazel, J.R. Bowen, R.A. Jensen, Arogenate (pretyrosine) is an obligatory intermediate of *L*-tyrosine biosynthesis: confirmation in a microbial mutant, Proc. Natl. Acad. Sci. U.S.A. 77 (1980) 1270–1273.
[34] P. Subramaniam, R. Bhatnagar, A. Hooper, R.A. Jensen, The dynamic progression of evolved character states for aromatic amino acid biosynthesis in gram-negative bacteria, Microbiol. 140 (1994) 3431–3440.
[35] D.E.A. Catcheside, Prephenate dehydrogenase from *Neurospora*: feedback activation by phenylalanine, Biochem. Biophys. Res. Commun. 36 (1969) 651–656.
[36] T. Lütke-Eversloh, G. Stephanopoulos, Feedback inhibition of chorismate mutase/prephenate dehydrogenase (TyrA) of *Escherichia coli*: generation and characterization of tyrosine-insensitive mutants, Appl. Environ. Microbiol. 71 (2005) 2774–7228.
[37] C.G. Friedrich, B. Friedrich, H.G. Schlegel, Regulation of chorismate mutase prephenate dehydratase and prephenate dehydrogenase from *Alcaligenes eutrophus*, J. Bacteriol. 126 (1976) 723–732.
[38] E. Blumenstock, O. Salcher, F. Lingens, Regulation of phenylalanine and tyrosine biosynthesis in *Pseudomonas aureofaciens*, J. Gen. Microbiol. 117 (1980) 81–87.
[39] H. Hagino, K. Nakayama, Regulatory properties of prephenate dehydrogenase and prephenate dehydratase from *Corynebacterium glutamicum*, Agric. Biol. Chem. 38 (1974) 2367–2376.
[40] A.M. Fazel, R.A. Jensen, Obligatory biosynthesis of *L*-tyrosine via the pretyrosine branchlet in coryneform bacteria, J. Bacteriol. 138 (1979) 805–815.
[41] R. Bode, C. Melo, D. Birnbaum, Regulation of chorismate mutase, prephenate dehydrogenase and prephenate dehydratase of *Candida maltosa*, J. Basic Microbiol. 25 (1985) 291–298.
[42] H.U.F. Lingens, W. Goebel, Regulation der Biosynthese der aromatischen Aminosauren in *Saccharomyces cerevisiae* 2. Repression, induktion und aktivierung, FEBS J. 1 (1967) 363–374.
[43] F. Lingens, W. Goebel, Regulation der biosynthese der aromatischen aminosäuren in *Claviceps paspali*, FEBS J. 2 (1967) 442–447.
[44] G. Mannhaupt, R. Stucka, U. Pilz, C. Schwarzlose, H. Feldmann, Characterization of the prephenate dehydrogenase-encoding gene, TYR1, from S*accharomyces cerevisiae*, Gene 85 (1989) 303–311.
[45] D. Botstein, S.A. Chervitz, J.M. Cherry, Yeast as a model organism, Science 277 (1997) 1259–1260.
[46] H. Karathia, E. Vilaprinyo, A. Sorribas, R. Alves, *Saccharomyces cerevisiae* as a model organism: a comparative study, PLoS One 6 (2011) e16015.
[47] E. Fernández-Fueyo, F.J. Ruiz-Dueñas, M.F. López-Lucendo, M. Pérez-Boada, J. Rencoret, A. Gutiérrez, A.G. Pisabarro, L. Ramírez, A.T. Martínez, A secretomic view of woody and nonwoody lignocellulose degradation by *Pleurotus ostreatus*, Biotechnol. Biofuels 9 (2016) 49.
[48] D. Feldman, D.J. Kowbel, N.L. Glass, O. Yarden, Y. Hadar, Detoxification of 5-hydroxymethylfurfural by the *Pleurotus ostreatus* lignolytic enzymes aryl alcohol oxidase and dehydrogenase, Biotechnol. Biofuels 8 (2015) 63.
[49] Q. Xiao, F. Ma, Y. Li, H. Yu, C. Li, X. Zhang, Differential proteomic profiles of *Pleurotus ostreatus* in response to lignocellulosic components provide insights into divergent adaptive mechanisms, Front. Microbiol. 8 (2017) 480.
[50] K. Tamura, G. Stecher, D. Peterson, A. Filipski, S. Kumar, MEGA6: molecular evolutionary genetics analysis version 6.0, Mol. Biol. Evol. 30 (2013) 2725–2729.
[51] R.C. Edgar, MUSCLE: multiple sequence alignment with high accuracy and high throughput, Nucleic Acids Res. 32 (2004) 1792–1797.
[52] J. Li, C. Tang, C. Song, M. Chen, Z. Feng, Y. Pan, A simple, rapid and effective method for total RNA extraction from *Lentinula edodes*, Biotechnol. Lett. 28 (2006) 1193–1197.
[53] J. Yang, Y. Zhang, I-TASSER server: new development for protein structure and function predictions, Nucleic Acids Res. 43 (2015) W174–W181.
[54] A. Roy, A. Kucukural, Y. Zhang, I. Tasser, A unified platform for automated protein structure and function prediction, Nat. Protoc. 5 (2010) 725–738.
[55] C.A. Bonner, T. Disz, K. Hwang, J. Song, V. Vonstein, R. Overbeek, R.A. Jensen, Cohesion group approach for evolutionary analysis of TyrA, a protein family with wide-ranging substrate specificities, Microbiol. Mol. Biol. Rev. 72 (2008) 13–53.
[56] C. Dornfeld, A.J. Weisberg, R.K. C, N. Dudareva, J.G. Jelesko, H.A. Maeda, Phylobiochemical characterization of class-Ib aspartate/prephenate aminotransferases reveals evolution of the plant arogenate phenylalanine pathway, Plant Cell 26 (2014) 3101–3114.
[57] J. Choi, S.-H. Kim, A genome Tree of life for the fungi kingdom, Proc. Natl. Acad. Sci. 114 (2017) 9391–9396.
[58] S. Chen, S. Vincent, D.B. Wilson, B. Ganem, Mapping of chorismate mutase and prephenate dehydrogenase domains in the *Escherichia coli* T-protein, Eur. J. Biochem. 270 (2003) 757–763.
[59] E. Heyde, Kinetic studies on the reactions catalyzed by chorismate mutase-prephenate dehydrogenase from *Aerobacter aerogenes*, Biochemistry 17 (1978) 1573–1580.
[60] N. Martins, C.L. Roriz, P. Morales, L. Barros, I.C.F.R. Ferreira, Coloring attributes of betalains: a key emphasis on stability and future applications, Food Funct 8 (2017) 1357–1372.
[61] W. Sun, D. Shahinas, J. Bonvin, W. Hou, M.S. Kimber, J. Turnbull, D. Christendat, The crystal structure of *Aquifex aeolicus* prephenate dehydrogenase reveals the mode of tyrosine inhibition, J. Biol. Chem. 284 (2009) 13223–13232.
[62] G.S. Byng, A. Berry, R.A. Jensen, Evolution of aromatic biosynthesis and fine-tuned phylogenetic positioning of Azomonas, Azotobacter and rRNA group I pseudomonads, Arch. Microbiol. 144 (1986) 222–227.
[63] W. Sun, S. Singh, R. Zhang, J.L. Turnbull, D. Christendat, Crystal structure of prephenate dehydrogenase from Aquifex aeolicus: insights into the catalytic mechanism, J. Biol. Chem. 18 (2006) 12919–12928.
[64] I. Shalaifer, J.L. Turnbull, Characterization of two key enzymes for aromatic amino acid biosynthesis in symbiotic archaea, Extremophiles 20 (2016) 503–514.
[65] D. Christendat, V.C. Saridakis, J.L. Turnbull, Use of site-directed mutagenesis to identify residues specific for each reaction catalyzed by chorismate mutase-prephenate dehydrogenase from *Escherichia coli*, Biochemistry 37 (1998) 15703–15712.
[66] K. Thodey Galanie, I.J. Trenchard, V. Filsinger Interrante, C.D. Smolke, Complete biosynthesis of opioids in yeast, Science 349 (2015) 1095–1100.
[67] C. Owen, N.J. Patron, A. Huang, A. Osbourn, Harnessing plant metabolic diversity, Curr. Opin. Chem. Biol. 40 (2017) 4–30.
[68] K. Thodey, S. Galanie, C.D. Smolke, A microbial biomanufacturing platform for natural and semisynthetic opioids, Nat. Chem. Biol. 10 (2014) 837–844.
[69] C.J. Paddon, P.J. Westfall, D.J. Pitera, K. Benjamin, K. Fisher, D. McPhee, M.D. Leavell, A. Tai, A. Main, D. Eng, D.R. Polichuk, K.H. Teoh, D.W. Reed, T. Treynor, J. Lenihan, H. Jiang, M. Fleck, S. Bajad, G. Dang, D. Dengrove, D. Diola,

G. Dorin, K.W. Ellens, S. Fickes, J. Galazzo, S.P. Gaucher, T. Geistlinger, R. Henry, M. Hepp, T. Horning, T. Iqbal, L. Kizer, B. Lieu, D. Melis, N. Moss, R. Regentin, S. Secrest, H. Tsuruta, R. Vazquez, L.F. Westblade, L. Xu, M. Yu, Y. Zhang, L. Zhao, J. Lievense, P.S. Covello, J.D. Keasling, K.K. Reiling, N.S. Renninger, J.D. Newman, High-level semi-synthetic production of the potent antimalarial artemisinin, Nature 469 (2013) 528–532.

[70] W.C. Deloache, Z.N. Russ, L. Narcross, A.M. Gonzales, V.J.J. Martin, J.E. Dueber, An enzyme-coupled biosensor enables (S)-reticuline production in yeast from glucose, Nat. Chem. Biol. 11 (2015) 465–471.

[71] A. Rodriguez, K.R. Kildegaard, M. Li, I. Borodina, J. Nielsen, Establishment of a yeast platform strain for production of p-coumaric acid through metabolic engineering of aromatic amino acid biosynthesis, Metab. Eng. 31 (2015) 181–188.

[72] P.S. Grewal, C. Modavi, Z.N. Russ, N.C. Harris, J.E. Dueber, Bioproduction of a betalain color palette in *Saccharomyces cerevisiae*, Metab. Eng. 45 (2018) 180–188.

[73] S.Y. Shin, S.M. Jung, M.D. Kim, N.S. Han, J.H. Seo, Production of resveratrol from tyrosine in metabolically engineered *Saccharomyces cerevisiae*, Enzym. Microb. Technol. 51 (2012) 211–216.

[74] Pickens, Y. Tang, Y.-H. Chooi, Metabolic engineering for the production of natural products, Annu. Rev. Chem. Biomol. Eng. 2 (2011) 211–236.